

Research Article

The Influence of Codopant Aluminum Ions (Al^{3+}) on the Optical Characteristics of $\text{YBO}_3:\text{Sm}^{3+}$ Phosphors

Hao-Ying Lu and Yi-Shao Chen

Department of Electronic Engineering, National Quemoy University, Kinmen 89250, Taiwan

Correspondence should be addressed to Hao-Ying Lu; hylu@nqu.edu.tw

Received 29 September 2014; Accepted 24 November 2014

Academic Editor: Silvia Licoccia

Copyright © 2015 H.-Y. Lu and Y.-S. Chen. This is an open access article distributed under the Creative Commons Attribution License, which permits unrestricted use, distribution, and reproduction in any medium, provided the original work is properly cited.

The yttrium borate (YBO_3) phosphors with codopants Al^{3+} and Sm^{3+} ions were prepared via the chemical coprecipitation method with one-hour thermal treatment at 1200°C . From the XRD patterns, the codopant Al^{3+} does not change the crystal structures of $\text{YBO}_3:\text{Sm}^{3+}$ and these patterns indicate that the phosphors crystallize as the hexagonal structure. Besides, the codopant Al^{3+} does not affect the wavelengths of emission bands but enhances the PL intensities of emission bands. Under the wavelength 406 nm excitation source, the emission peaks locating at wavelengths 571 nm, 611 nm, and 657 nm are assigned to the electronic transitions $^4\text{G}_{5/2} \rightarrow ^6\text{H}_{5/2}$, $^4\text{G}_{5/2} \rightarrow ^6\text{H}_{7/2}$, and $^4\text{G}_{5/2} \rightarrow ^6\text{H}_{9/2}$, respectively. The PL intensities of phosphors $\text{Sm}_{0.01}\text{Al}_x\text{Y}_{0.99-x}\text{BO}_3$ increase with the Al^{3+} ion concentration. As the concentration of Al^{3+} ions increases to 3%, the PL intensity of $\text{Sm}_{0.01}\text{Al}_x\text{Y}_{0.99-x}\text{BO}_3$ phosphor reaches its maximum intensity. When the concentration of Al^{3+} ions is above 3%, the PL intensity of phosphor $\text{Sm}_{0.01}\text{Al}_x\text{Y}_{0.99-x}\text{BO}_3$ decreases. Comparing with the $\text{Sm}_{0.01}\text{Y}_{0.99}\text{BO}_3$ phosphor, the PL intensity locating at wavelength 571 nm of $\text{Sm}_{0.01}\text{Al}_{0.03}\text{Y}_{0.96}\text{BO}_3$ phosphor is about 1.8 times stronger than the $\text{Sm}_{0.01}\text{Y}_{0.99}\text{BO}_3$ phosphor. It is believed that the codopant Al^{3+} can improve the luminescent characteristics of $\text{YBO}_3:\text{Sm}^{3+}$ phosphors.

1. Introduction

In the past, plasma display panels (PDPs) were applied to full-color large-area flat panel displays because of their high performance and scalability [1, 2]. Phosphors play an important role in PDPs and they are usually stimulated by vacuum ultraviolet (VUV) light (145–180 nm) generated by the discharge of Xe or Ne gas [3]. In recent years, the phosphors have attracted more attentions due to their extensive applications in light emitting diodes (LEDs). Compared with the PDPs, the LEDs possess several advantages, such as the longer lifetime, lower energy consumption, higher efficiency, and higher brightness [4–6]. The advantages above make LEDs be important lighting devices in recent years. Owing to the excellent power-saving property (compared with the traditional lighting devices, such as the incandescent bulbs and fluorescent lamps), people put much effort to fabricate the white-light emitting diodes (WLEDs). Combining the emissions of red-light, green-light, and blue-light phosphors is a method to fabricate the WLEDs [7]. However, it is very

difficult to control the color purity accurately with three phosphors. Combination of a blue-light LED chip and a yellow-light phosphor is most widely used in fabricating WLEDs [8] and this method reveals the importance of yellow-light phosphors.

In the present studies, oxides, including aluminates, borates, and silicates, could be used as the host materials due to the strong absorption of the VUV light [9]. The strong absorption can enhance the PL intensity effectively. In our previous work, the $\text{YBO}_3:\text{Sm}^{3+}$ phosphors were synthesized to replace the YAG phosphors to fabricate the WLEDs and in fact they can emit orange-yellow light. But the emitting intensities of $\text{YBO}_3:\text{Sm}^{3+}$ phosphors are too weak to be used in the WLEDs. In order to enhance the emitting intensity, the sensitizers are usually used to codope with the host materials [10]. In Kwon et al.'s research, the addition of sensitizer is an effective method to improve the optical properties of phosphor [11, 12]. In this paper, the Al^{3+} is chosen as the sensitizer to codope with the $\text{YBO}_3:\text{Sm}^{3+}$ phosphors to form the $\text{Sm}_{0.01}\text{Al}_x\text{Y}_{0.99-x}\text{BO}_3$ phosphors (x starts from

0 to 0.05). As the concentration of Al^{3+} increases to 3% ($\text{Sm}_{0.01}\text{Al}_{0.03}\text{Y}_{0.96}\text{BO}_3$), the PL intensity is about 1.8 times stronger than the $\text{Sm}_{0.01}\text{Y}_{0.99}\text{BO}_3$ phosphors.

2. Materials and Methods

The $\text{YBO}_3\text{:Sm}^{3+}$ and $\text{YBO}_3\text{:Sm}^{3+}, \text{Al}^{3+}$ phosphors were synthesized via the chemical coprecipitation method with one-hour thermal treatment at 1200°C . Samarium nitrate hexahydrate $\text{Sm}(\text{NO}_3)_3 \cdot 6\text{H}_2\text{O}$ (99.9%, Alfa Aesar), yttrium nitrate hexahydrate $\text{Y}(\text{NO}_3)_3 \cdot 6\text{H}_2\text{O}$ (99.9%, Alfa Aesar), aluminum nitrate nonahydrate $\text{Al}(\text{NO}_3)_3 \cdot 9\text{H}_2\text{O}$ (>98%, Panreac), and boric acid H_3BO_3 (99.8%, Panreac) were used as the starting materials to prepare the precursor solutions. $\text{Sm}(\text{NO}_3)_3 \cdot 6\text{H}_2\text{O}$, $\text{Y}(\text{NO}_3)_3 \cdot 6\text{H}_2\text{O}$, $\text{Al}(\text{NO}_3)_3 \cdot 9\text{H}_2\text{O}$, and H_3BO_3 were dissolved into distilled water separately according to the stoichiometric ratio. Then, the solutions above were mixed together and stirred for an hour at room temperature. After stirring, 1% ammonia solution was used as the precipitant and added to the solution mentioned above. With the addition of ammonia, the pH value of mixed solution was adjusted to 9.0, and this solution was placed for an hour. After an hour, the white precipitation could be observed and separated directly by a centrifuge. This white precipitation was washed repeatedly with distilled water and ethanol to remove the impurities and then dried at 70°C for 12 hours. Finally, the dried precipitation was grinded for 15 minutes and used as the precursor to synthesize the $\text{Sm}_{0.01}\text{Y}_{0.99}\text{BO}_3$ and $\text{Sm}_{0.01}\text{Al}_x\text{Y}_{0.99-x}\text{BO}_3$ phosphors via the suitable thermal treatment in the air atmosphere for an hour.

The crystal structures of phosphors were characterized by Rigaku Miniflex II desktop X-ray diffractometer with $\text{CuK}\alpha$ radiation (θ : 10° to 40° , step: 0.01°). The size of the particle and morphology of prepared phosphors were investigated by using a field-emission scanning electron microscope (FE-SEM, Hitachi S4100) with 15 KV accelerating voltage. And the PL spectra and the PLE spectra were examined with a fluorescence spectrophotometer (Hitachi F-2700). All the measurements were carried out at room temperature.

3. Results and Discussion

The XRD patterns of the $\text{Sm}_{0.01}\text{Al}_x\text{Y}_{0.99-x}\text{BO}_3$ (x starts from 0 to 0.05) phosphors annealed at 1200°C are shown in Figure 1. Comparing with the JCPDS card, all peaks are consistent with the number 16-0277 pattern and they exhibit a pure hexagonal phase with vaterite-type structure. These patterns prove that the codopant Al^{3+} does not cause the transformation of the crystal structure. According to the Scherrer formula, the average size of the particle in diameter can be calculated by the FWHM of (1 0 0) peak. Here, the Scherrer formula is shown as follows:

$$D = \frac{0.9\lambda}{\beta \cos \theta}, \quad (1)$$

where D is the average particle size, λ is the wavelength of X-ray radiation (1.54\AA), β is the full width at half maximum (FWHM), and θ is the diffraction peak angle. The average

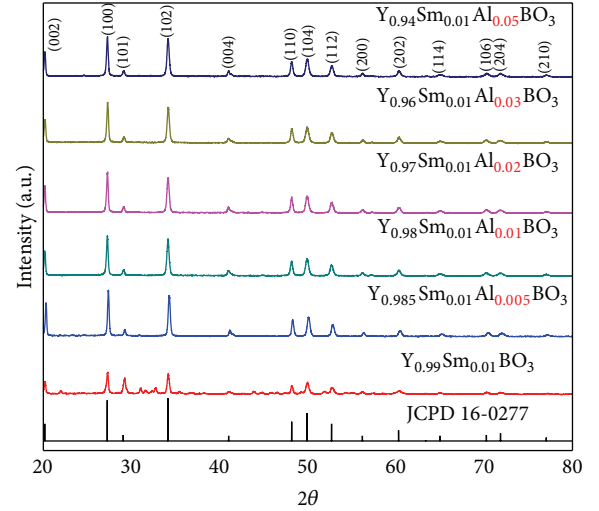


FIGURE 1: The XRD patterns of the $\text{Sm}_{0.01}\text{Al}_x\text{Y}_{0.99-x}\text{BO}_3$ phosphors ($0 \leq x \leq 0.05$) annealed at 1200°C for 1 hour.

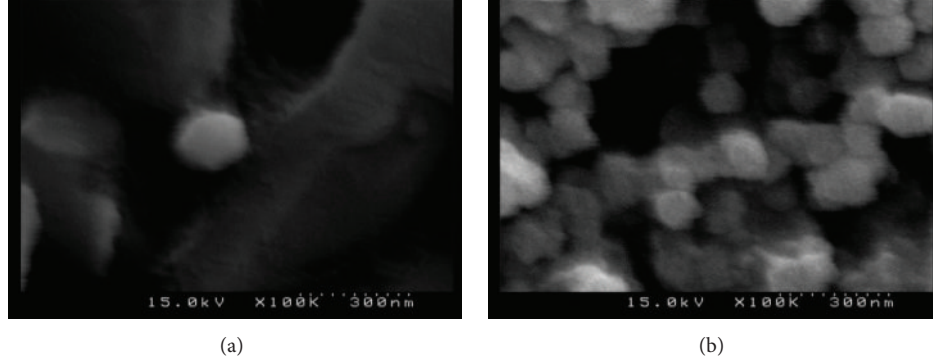
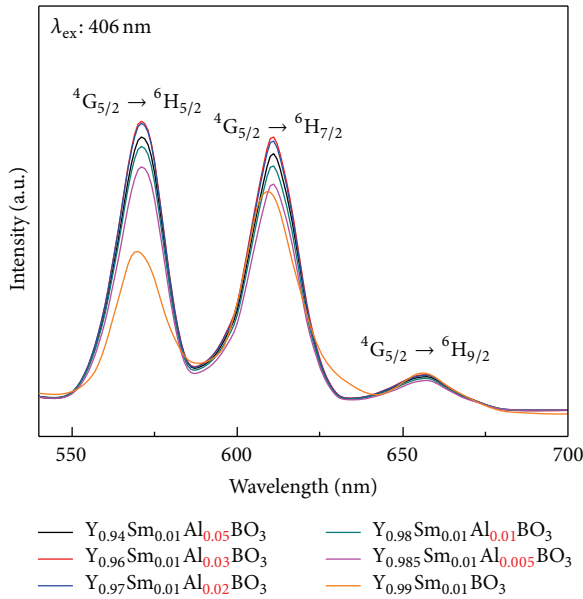
particle sizes calculated by the Scherrer formula are shown in Table 1. Referring to Figure 2, the calculated results are similar to the exact sizes of particle.

Figure 2 shows the images of surface morphology of the $\text{Sm}_{0.01}\text{Y}_{0.99}\text{BO}_3$ and $\text{Sm}_{0.01}\text{Al}_{0.03}\text{Y}_{0.96}\text{BO}_3$ phosphors. From Figures 2(a) and 2(b), the codopant Al^{3+} does not really influence the particle sizes and shapes. The FE-SEM images show that the prepared phosphors are spherical and the sizes of the particle are between 100 and 200 nm. These sizes of particle are consistent with the XRD results. In addition, the spherical morphology of phosphors synthesized by the method in this paper has several advantages, including the high packing densities, good slurry properties, and smoother light intensity distributions [13].

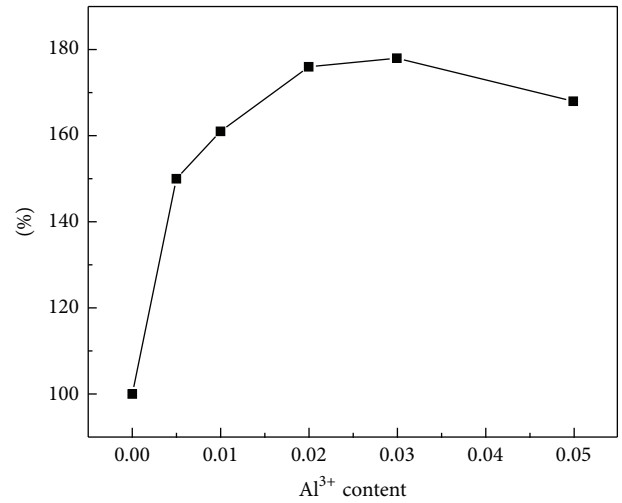
In our previous work, the YBO_3 phosphor with 1% Sm^{3+} possesses the strongest PL intensity. In order to enhance the PL intensity of $\text{YBO}_3\text{:Sm}^{3+}$ phosphors and prevent the concentration-quenching effect of activator, the sensitizer Al^{3+} is used to codope with the $\text{YBO}_3\text{:Sm}^{3+}$ phosphors. The emission spectra of the $\text{Sm}_{0.01}\text{Al}_x\text{Y}_{0.99-x}\text{BO}_3$ ($0 \leq x \leq 0.05$) phosphors with the excitation wavelength 406 nm are shown in Figure 3. The emission peaks locating at wavelengths 571, 611, and 657 nm appear because of the following transitions $^4\text{G}_{5/2} \rightarrow ^6\text{H}_{5/2}$, $^4\text{G}_{5/2} \rightarrow ^6\text{H}_{7/2}$, and $^4\text{G}_{5/2} \rightarrow ^6\text{H}_{9/2}$, respectively [14]. The peak locating at 657 nm is too weak to dominate the color coordinates and these phosphors can yield the orange-yellow light. Besides, from these emission spectra, the codopant Al^{3+} does not actually affect the emission wavelength but it really influences the intensity of PL emission. From Figure 4, the emission intensity of phosphor increases with the Al^{3+} concentration. As the Al^{3+} concentration increases to 3%, the $\text{Sm}_{0.01}\text{Al}_{0.03}\text{Y}_{0.96}\text{BO}_3$ phosphor possesses the strongest PL intensity. The addition of sensitizers Al^{3+} leads to a significant increment of the PL emission intensity because the sensitizer Al^{3+} ions absorb the excitation energy and transfer the energy to the Sm^{3+}

TABLE 1: The average particle sizes of $\text{Sm}_{0.01}\text{Al}_x\text{Y}_{0.99-x}\text{BO}_3$ phosphors with different Al^{3+} concentrations.

The average particle size of $\text{Sm}_{0.01}\text{Al}_x\text{Y}_{0.99-x}\text{BO}_3$ phosphors						
Al^{3+} concentration	0%	0.5%	1%	2%	3%	5%
Particle size (nm)	96	107	112	106	99	102

FIGURE 2: The FE-SEM images of (a) $\text{Sm}_{0.01}\text{Y}_{0.99}\text{BO}_3$ and (b) $\text{Sm}_{0.01}\text{Al}_{0.03}\text{Y}_{0.96}\text{BO}_3$ phosphors annealed at 1200°C for 1 hour.FIGURE 3: The emission spectra of the $\text{Sm}_{0.01}\text{Al}_x\text{Y}_{0.99-x}\text{BO}_3$ ($0 \leq x \leq 0.05$) phosphors annealed at 1200°C for 1 hour.

ions through the host lattice [15]. Moreover, the excitation energy absorbed by the Y^{3+} ions and BO_3^{3-} groups may be transferred nonradiatively to the Al^{3+} ions and then to the Sm^{3+} ions. Another research team believes that the nonradiative transfer mechanism, the resonance between absorber and emitter, dominates the enhancement as well [16]. When the concentration of Al^{3+} is above 3%, the PL intensity decreases. This phenomenon reveals that the energy transfer not only occurs between the sensitizers and activators but also occurs within the sensitizers. As the concentration of Al^{3+} ions increases over 3%, the distance between Al^{3+} ions would be small enough, and the excitation energy absorbed by the Al^{3+} ions tends to transfer within the Al^{3+} ions rather than

FIGURE 4: The peak intensities of $\text{Sm}_{0.01}\text{Al}_x\text{Y}_{0.99-x}\text{BO}_3$ phosphors with different Al^{3+} concentrations.

transfer between Al^{3+} and Sm^{3+} [17]. Except the radiative relaxation, the energy of the activator Sm^{3+} can release through a nonradiative transition instead of orange emission [15]. Figure 5 shows the mechanism mentioned above. The probability of path A increases with the concentration of Al^{3+} ions and dominates the mechanism of energy transfer till the concentration of Al^{3+} increases to 3%. When the concentration of Al^{3+} ions is above 3%, the path B dominates the energy transfer and results in the decrease of PL intensity.

The excitation spectra of $\text{Sm}_{0.01}\text{Al}_x\text{Y}_{0.99-x}\text{BO}_3$ ($0 \leq x \leq 0.05$) phosphors are shown in Figures 6 and 7. Figure 6 shows the PLE spectra of $\text{Sm}_{0.01}\text{Al}_{0.03}\text{Y}_{0.96}\text{BO}_3$ phosphor with different emission wavelengths. The wavelengths of all absorption peaks are the same, and the intensity ratios of absorption peaks are similar as well. Ten absorption peaks can be observed in Figure 7 and these ten peaks overlap with each

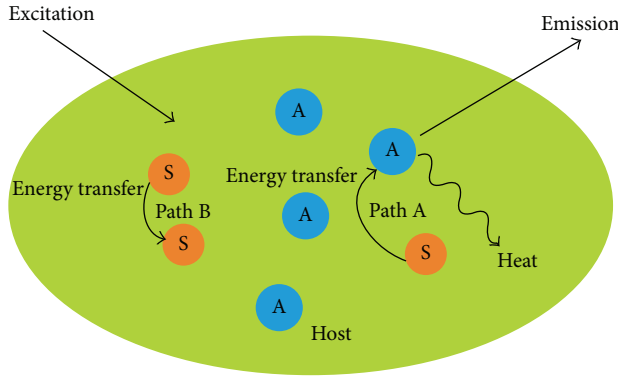


FIGURE 5: The mechanism of energy transfer in the $\text{YBO}_3:\text{Sm}^{3+}, \text{Al}^{3+}$ phosphor. A means activator and S means sensitizer.

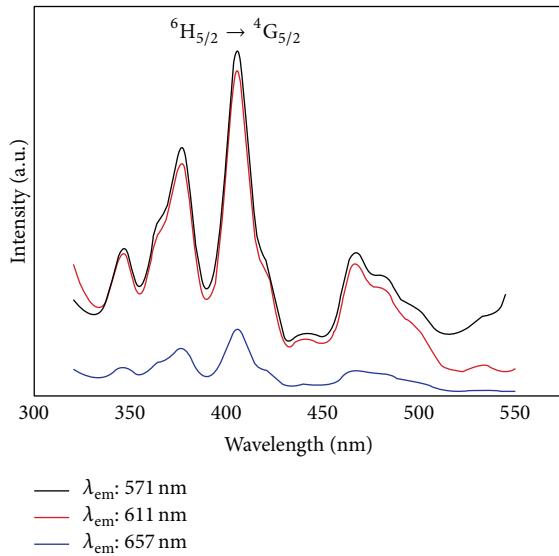


FIGURE 6: The excitation spectra of $\text{Sm}_{0.01}\text{Al}_{0.03}\text{Y}_{0.96}\text{BO}_3$ phosphor with different emission wavelengths.

other to form four absorption bands. The 406 nm absorption peak locating at the third absorption band is the strongest peak of all and is chosen as the excitation wavelength for the PL measurements. This strongest absorption is the result of the following transition ${}^6\text{H}_{5/2} \rightarrow {}^4\text{K}_{11/2}$ [18]. From the PLE spectra, the $\text{YBO}_3:\text{Sm}^{3+}$ phosphor with 3% Al^{3+} can absorb the more energy and this phenomenon is consistent with the PL spectra.

Figure 8 shows the Commission Internationale de l'Eclairage (CIE) chromaticity diagram of the $\text{Sm}_{0.01}\text{Y}_{0.99}\text{BO}_3$ and $\text{Sm}_{0.01}\text{Al}_{0.03}\text{Y}_{0.96}\text{BO}_3$ phosphors. The color coordinates of $\text{YBO}_3:\text{Sm}^{3+}$ phosphor and $\text{YBO}_3:\text{Sm}^{3+}, \text{Al}^{3+}$ phosphor are (0.542, 0.457) and (0.531, 0.467), respectively. From the CIE diagram, the emission colors of these two phosphors locate at the orange-yellow light area. With the addition of Al^{3+} ions, the color coordinate shifts toward the yellow-light area. Referring to the PL emission spectra, the sensitizer Al^{3+} enhances the emission intensity of 571 nm peak mostly

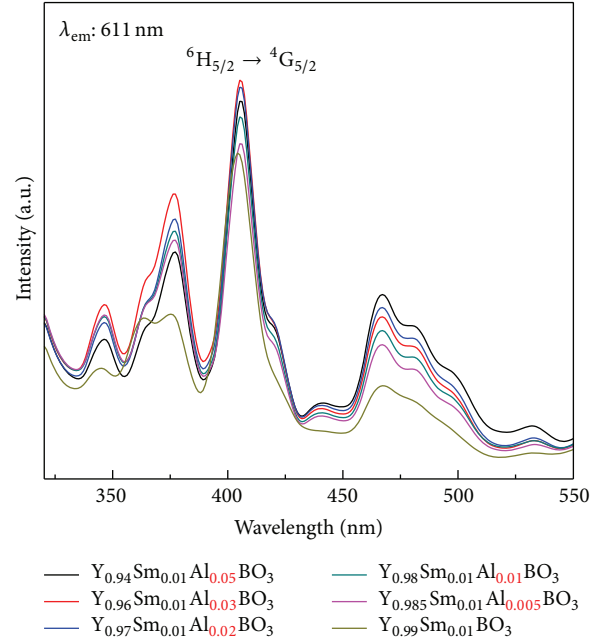


FIGURE 7: The excitation spectra of $\text{Sm}_{0.01}\text{Al}_x\text{Y}_{0.99-x}\text{BO}_3$ ($0 \leq x \leq 0.05$) phosphors annealed at 1200°C for 1 hour.

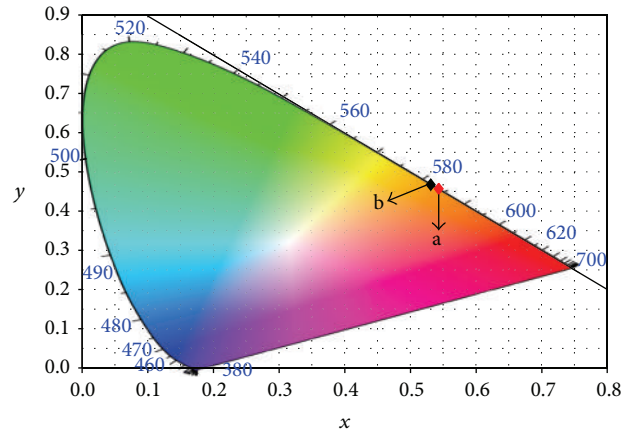


FIGURE 8: The CIE chromaticity diagram of (a) $\text{Sm}_{0.01}\text{Y}_{0.99}\text{BO}_3$ and (b) $\text{Sm}_{0.01}\text{Al}_{0.03}\text{Y}_{0.96}\text{BO}_3$ phosphors annealed at 1200°C for 1 hour.

and changes the intensity ratio of 571 nm peak and 611 nm peak. This mechanism leads to the change of chromaticity.

4. Conclusion

The nanosized $\text{YBO}_3:\text{Sm}^{3+}, \text{Al}^{3+}$ phosphors can be obtained via the chemical coprecipitation method. With the thermal treatment at 1200°C for 1 hour, the average size of particle is between 100 and 200 nm and it is consistent with the result calculated by the Scherrer formula. The synthesized phosphors exhibit the spherical morphology and can emit the orange-yellow light. From the XRD patterns, the addition of sensitizer Al^{3+} does not affect the crystal structure and all the $\text{Sm}_{0.01}\text{Al}_x\text{Y}_{0.99-x}\text{BO}_3$ phosphors crystallize as the hexagonal

phase with vaterite-type structure. With the excitation wavelength 406 nm, the $\text{Sm}_{0.01}\text{Al}_x\text{Y}_{0.99-x}\text{BO}_3$ phosphors can emit three emission bands. The emission peaks locating at wavelengths 571, 611, and 657 nm are the results of the following transitions $^4\text{G}_{5/2} \rightarrow ^6\text{H}_{5/2}$, $^4\text{G}_{5/2} \rightarrow ^6\text{H}_{7/2}$, and $^4\text{G}_{5/2} \rightarrow ^6\text{H}_{9/2}$, respectively. From the PL spectra, the emission intensity of $\text{Sm}_{0.01}\text{Al}_x\text{Y}_{0.99-x}\text{BO}_3$ phosphor increases with the Al^{3+} concentration. As the Al^{3+} concentration increases to 3%, the $\text{Sm}_{0.01}\text{Al}_{0.03}\text{Y}_{0.96}\text{BO}_3$ phosphor possesses the strongest PL intensity. The addition of sensitizer Al^{3+} does not influence the emission wavelengths but enhances the emission intensity of 571 nm peak. Comparing with the $\text{Sm}_{0.01}\text{Y}_{0.99}\text{BO}_3$ phosphor, the PL intensity locating at wavelength 571 nm of $\text{Sm}_{0.01}\text{Al}_{0.03}\text{Y}_{0.96}\text{BO}_3$ phosphor is about 1.8 times stronger than the Al^{3+} -free phosphor. This phenomenon leads to the change of intensity ratio and shifts the CIE coordinate to the yellow-light area. This result indicates that the codopant Al^{3+} can improve the optical characteristics of $\text{YBO}_3:\text{Sm}^{3+}$ phosphors effectively.

Conflict of Interests

The authors declare that there is no conflict of interests regarding the publication of this paper.

References

- [1] M. Ferhi, K. Horchani-Naifer, and M. Férid, "Hydrothermal synthesis and photoluminescence of the monophosphate $\text{LaPO}_4:\text{Eu}(5\%)$," *Journal of Luminescence*, vol. 128, no. 11, pp. 1777–1782, 2008.
- [2] U. Rambabu and S. Buddhudu, "Optical properties of $\text{LnPO}_4:\text{Eu}^{3+}$ ($\text{Ln} = \text{Y}, \text{La}$ and Gd) powder phosphors," *Optical Materials*, vol. 17, no. 3, pp. 401–408, 2001.
- [3] W. Di, X. Wang, B. Chen, H. Lai, and X. Zhao, "Preparation, characterization and VUV luminescence property of $\text{YPO}_4:\text{Tb}$ phosphor for a PDP," *Optical Materials*, vol. 27, no. 8, pp. 1386–1390, 2005.
- [4] H. A. Höppe, "Recent developments in the field of inorganic phosphors," *Angewandte Chemie International Edition*, vol. 48, no. 20, pp. 3572–3582, 2009.
- [5] S. Ye, F. Xiao, Y. X. Pan, Y. Y. Ma, and Q. Y. Zhang, "Phosphors in phosphor-converted white light-emitting diodes: recent advances in materials, techniques and properties," *Materials Science and Engineering: R: Reports*, vol. 71, no. 1, pp. 1–34, 2010.
- [6] M. Upasani, B. Butey, and S. V. Moharil, "Luminescence studies on lanthanide ions (Gd^{3+} , Tb^{3+}) doped $\text{YAG}:\text{Ce}$ phosphors by combustion synthesis," *Journal of Applied Physics*, vol. 6, no. 2, pp. 28–33, 2014.
- [7] Y. Ji, J. Cao, Z. Zhu, J. Li, Y. Wang, and C. Tu, "Synthesis and white light emission of Dy^{3+} ions doped hexagonal structure YAlO_3 nanocrystalline," *Journal of Luminescence*, vol. 132, no. 3, pp. 702–706, 2012.
- [8] G. Blasse and A. Brill, "Investigation of some Ce^{3+} -activated phosphors," *The Journal of Chemical Physics*, vol. 47, p. 5139, 1967.
- [9] Z.-J. Zhang, J.-L. Yuan, S. Chen et al., "Investigation on the luminescence of RE^{3+} ($\text{RE} = \text{Ce}, \text{Tb}, \text{Eu}$ and Tm) in $\text{KMg}(\text{PO}_4)_2$ ($\text{M} = \text{Ca}, \text{Sr}$) phosphates," *Optical Materials*, vol. 30, no. 12, pp. 1848–1853, 2008.
- [10] K. Park, J. Kim, and K. Y. Kim, "Enhancement of green emission for Al^{3+} -doped $\text{YBO}_3:\text{Tb}^{3+}$," *Materials Chemistry and Physics*, vol. 136, no. 1, pp. 264–267, 2012.
- [11] I.-E. Kwon, B.-Y. Yu, H. Bae et al., "Luminescence properties of borate phosphors in the UV/VUV region," *Journal of Luminescence*, vol. 87–89, pp. 1039–1041, 2000.
- [12] K. Park and S. W. Nam, "Red-emitting $(\text{Y}_{0.5}\text{Gd}_{0.5})_{0.94-x}\text{Al}_x\text{Eu}_{0.06}\text{VO}_4$ ($0 \leq x \leq 0.04$) phosphors for plasma display panel applications," *Optical Materials*, vol. 32, no. 5, pp. 612–615, 2010.
- [13] H. S. Roh, Y. C. Kang, H. D. Park, and S. B. Park, " $\text{Y}_2\text{O}_3:\text{Eu}$ phosphor particles prepared by spray pyrolysis from a solution containing citric acid and polyethylene glycol," *Applied Physics A: Materials Science and Processing*, vol. 76, no. 2, pp. 241–245, 2003.
- [14] S. Neeraj, N. Kijima, and A. K. Cheetham, "Novel red phosphors for solid state lighting: The system $\text{Bi}_x\text{Ln}_{1-x}\text{VO}_4:\text{Eu}^{3+}/\text{Sm}^{3+}$ ($\text{Ln} = \text{Y}, \text{Gd}$)," *Solid State Communications*, vol. 131, no. 1, pp. 65–69, 2004.
- [15] B. N. Mahalley, S. J. Dhoble, R. B. Pode, and G. Alexander, "Photoluminescence in $\text{GdVO}_4:\text{Bi}^{3+}$, Eu^{3+} red phosphor," *Applied Physics A: Materials Science and Processing*, vol. 70, no. 1, pp. 39–45, 2000.
- [16] W. Minquan, F. Xianping, and X. Guohong, "Luminescence of Bi^{3+} ions and energy transfer from Bi^{3+} ions to Eu^{3+} ions in silica glasses prepared by the sol-gel process," *Journal of Physics and Chemistry of Solids*, vol. 56, no. 6, pp. 859–862, 1995.
- [17] L. Chen, G. Yang, J. Liu, X. Shu, G. Zhang, and Y. Jiang, "Photoluminescence properties of Eu^{3+} and Bi^{3+} in YBO_3 host under vacuum ultraviolet/ultraviolet excitation," *Journal of Applied Physics*, vol. 105, no. 1, Article ID 013513, 2009.
- [18] V. Natarajan, A. R. Dhobale, and C.-H. Lu, "Preparation and characterization of tunable $\text{YVO}_4:\text{Bi}^{3+}$, Sm^{3+} phosphors," *Journal of Luminescence*, vol. 129, no. 3, pp. 290–293, 2009.

